THE JOURNAL OF BIOLOGICAL CHEMISTRY VOL. 285, NO. 36, pp. 28164–28173, September 3, 2010

Are Osteoclasts Needed for the Bone Anabolic Response to Parathyroid Hormone?

*A STUDY OF INTERMITTENT PARATHYROID HORMONE WITH DENOSUMAB OR ALENDRONATE IN KNOCK-IN MICE EXPRESSING HUMANIZED RANKL**[S]

Received for publication, January 7, 2010, and in revised form, June 1, 2010 Published, JBC Papers in Press, June 17, 2010, DOI 10.1074/jbc.M110.101964

Dominique D. Pierroz[‡], Nicolas Bonnet[‡], Paul A. Baldock[§], Michael S. Ominsky[¶], Marina Stolina[¶], Paul J. Kostenuik[¶], and Serge L. Ferrari[‡1]

From the [‡]Service of Bone Diseases, Department of Rehabilitation and Geriatrics, Geneva University Hospital and Faculty of Medicine, 1211 Geneva 14, Switzerland, the [§]Bone and Mineral Program, Garvan Institute of Medical Research, St. Vincent's Hospital, Sydney, New South Wales 2010, Australia, and the [¶]Metabolic Disorders Research, Amgen Inc., Thousand Oaks, California 91320

PTH stimulates osteoblastic cells to form new bone and to produce osteoblast-osteoclast coupling factors such as RANKL. Whether osteoclasts or their activity are needed for PTH anabolism remains uncertain. We treated ovariectomized huRANKL knock-in mice with a human RANKL inhibitor denosumab (DMAb), alendronate (Aln), or vehicle for 4 weeks, followed by co-treatment with intermittent PTH for 4 weeks. Loss of bone mass and microarchitecture was prevented by Aln and further significantly improved by DMAb. PTH improved bone mass, microstructure, and strength, and was additive to Aln but not to DMAb. Aln inhibited biochemical and histomorphometrical indices of bone turnover, -*i.e.* osteocalcin and bone formation rate (BFR) on cancellous bone surfaces-, and Dmab inhibited them further. However Aln increased whereas Dmab suppressed osteoclast number and surfaces. PTH significantly increased osteocalcin and bone formation indices, in the absence or presence of either antiresorptive, although BFR remained lower in presence of Dmab. To further evaluate PTH effects in the complete absence of osteoclasts, high dose PTH was administered to RANK$^{-/-}$ mice. PTH increased osteocalcin similarly in RANK$^{-/-}$ and WT mice. It also increased BMD in RANK$^{-/-}$ mice, although less than in WT. These results further indicate that osteoclasts are not strictly required for PTH anabolism, which presumably still occurs via stimulation of modeling-based bone formation. However the magnitude of PTH anabolic effects on the skeleton, in particular its additive effects with antiresorptives, depends on the extent of the remodeling space, as determined by the number and activity of osteoclasts on bone surfaces.

Parathyroid hormone (PTH),[2] when administered intermittently, increases bone mineral density (BMD) and improves bone microarchitecture and strength (1). PTH induces a rapid increase in markers of bone formation before it also increases bone resorption, which has been described as an "anabolic window" (2). In this window, PTH has been suggested to directly activate bone formation via bone lining cells on quiescent bone surfaces (*i.e.* modeling surfaces), as indicated by an increase in double tetracycline-labeled surfaces and a smooth cement line (3). PTH subsequently stimulates bone remodeling, first through activation of osteoclastic bone resorption in the basic multicellullar units (BMU), followed by new bone formation by osteoblasts. These remodeling-based BMUs are associated with scalloped cement lines by microscopy. Data from untreated adult rodents indicate that the ratio of bone modeling:remodeling surfaces is less than 1:5 and further decreases with age (4). Although PTH has been shown to increase bone modeling in rodents, the vast majority of bone formation in humans appears to be remodeling-based (5). Data from humans treated with PTH indicate that bone formation on modeling surfaces accounts for only 5–30% of PTH anabolic effects (6). While intermittent PTH can partially restore bone microarchitecture by increasing bone formation in modeling and remodeling osteons (5), it also stimulates Haversian bone remodeling leading to cortical porosity (7, 8). In contrast, antiresorptive therapies, such as bisphosphonates (*e.g.* alendronate (Aln)), inhibit bone remodeling and maintain, but do not restore, bone microarchitecture. These attributes have led to significant interest in the combination of PTH with antiresorptive agents. However, some clinical studies have failed to demonstrate an additive effect of PTH plus Aln on bone, at least when PTH treatment was initiated together with Aln (9–11). This outcome might suggest that when remodeling is suppressed by antiresorptive agents, the anabolic potential of intermittent PTH therapy is related to the extent of residual remod-

* This work was supported by Amgen Inc.
[S] The on-line version of this article (available at http://www.jbc.org) contains supplemental Table S1.
[1] To whom correspondence should be addressed: Service of Bone Diseases, Dept. of Rehabilitation and Geriatrics, HUGs, 4, rue Gabrielle-Perret-Gentil, 1211 Geneva 14. Tel.: 41-22-382-99-52; Fax: 41-22-382-99-73; E-mail: Serge.Ferrari@unige.ch.
[2] The abbreviations used are: PTH, parathyroid hormone; BMD, bone mineral density; BMU, basic multicellullar unit; Aln, alendronate; BMP, bone morphogenetic protein; M-CSF, macrophage colony stimulating factor; OPG, osteoprotegerin; rhOPG, recombinant form of human OPG; huRANKL, chimeric human/mouse RANKL; TRAP, tartrate-resistant acid phosphatase; DMAb, denosumab; OVX, ovariectomized; SC, subcutaneous; Veh, vehicle; micro-CT, micro-computed tomography; vBMD, trabecular volumetric BMD; pDXA, peripheral dual-energy x-ray absorptiometry; TB BMD, total body BMD; TRACP5b, serum tartrate-resistant acid phosphatase form 5b; MS, mineralizing surface; BS, bone surface; MAR, mineral apposition rate; BFR, bone formation rate; BV/TV, bone volume fraction; Tb N, trabecular number; Tb Th, thickness; OcS/BS, osteoclast surface; OcN, osteoclast number; Sh, sham.

eling space, and to the ability of PTH to stimulate modeling-based bone formation.

Although still incompletely understood, physiological coupling between osteoclasts and osteoblasts occurs through the complex actions of systemic hormones (12, 13), factors released by osteoclasts and/or from the bone matrix by resorption (*e.g.* TGF-β, IGF-I and II, and bone morphogenetic proteins (BMP)) (14), and direct cell-to-cell contact through ephrins and ephrin receptors on the cell surface (15–17). Pharmacologic coupling of osteoclasts to osteoblasts is also apparent with intermittent PTH administration and some evidence suggests that active resorption plays an important role (13–16). For example, PTH had no effects on bone microarchitecture in a patient with pycnodysostosis, a disease characterized by the presence of osteoclasts but suppressed bone resorption due to mutations in cathepsin K (18). Aln might provide a useful tool to test the hypothesis that active bone-resorbing osteoclasts are more important than the mere presence of osteoclasts for PTH anabolism because Aln can potently suppress osteoclast activity without necessarily reducing osteoclast numbers (12).

Osteoclast formation, activation, and survival require RANK and are stimulated by RANK ligand (RANKL) and macrophage colony-stimulating factor (M-CSF). Abundant evidence from knock-out and transgenic rodent models have demonstrated that inhibition of the RANK/RANKL pathway increases bone mass (19, 20), structure (21), and strength (22). Osteoblasts/stromal cells also produce osteoprotegerin (OPG), a soluble decoy receptor that prevents RANK activation by binding and sequestering RANKL. OPG negatively regulates osteoclastogenesis, promotes apoptosis of mature osteoclasts, and ultimately inhibits bone resorption (23). Hence, OPG-deficient mice exhibit increased bone turnover and reductions in cortical and trabecular bone volume, and they develop spontaneous fractures (24). In contrast, overexpression of OPG or soluble RANK-Fc (which functions as a RANKL inhibitor) in transgenic rodents inhibited bone remodeling and resulted in high bone mass (23, 25). Concomitant administration of OPG-Fc and PTH in rodents has shown additive effects on BMD (26, 27) despite evidence of blunting of bone formation relative to PTH alone (28). Importantly, after accounting for its antiremodeling effect, OPG did not reduce the magnitude by which PTH increased the bone formation marker osteocalcin (29). Moreover, OPG did not directly inhibit differentiation of cultured osteoblasts (28). These observations suggest that RANKL inhibitors may restrict PTH anabolism through their effects on bone remodeling rather than on bone-forming cells themselves. The effects of antiresorptives and PTH might further depend on the sequence and duration of exposure to the agents. PTH combined with Aln in rodents has generally led to additive effects on bone mass and structure, whereas bone formation parameters appear suppressed relative to PTH alone (27, 28, 30). These results further highlight the lack of clarity regarding the role of osteoclasts for PTH anabolic effects on bone.

We re-evaluated the role of osteoclasts and bone resorption on intermittent PTH effects on the skeleton in 2 mouse models. The first was a knock-in mouse model expressing a chimeric human/mouse RANKL protein (huRANKL), which was developed to respond to the neutralizing human monoclonal IgG2 against RANKL, denosumab (31). In this model, denosumab was expected to markedly reduce osteoclast numbers and bone remodeling, while Aln was expected to inhibit remodeling without reducing osteoclast numbers. Introducing PTH under these conditions could help to determine whether PTH anabolism is more related to osteoclast numbers or to their activity. However, PTH proved capable of somewhat increasing osteoclast numbers and bone formation parameters even in presence of high-dose denosumab. We therefore further examined whether PTH could stimulate bone formation and increase bone mass in mice that were virtually devoid of osteoclasts, *i.e.* RANK knock-out ($RANK^{-/-}$) mice (19, 32). Altogether our data indicate that PTH is still capable to stimulate bone formation when bone resorption is inhibited, however, the magnitude of PTH anabolic effects on the skeleton, in particular its additive effects with antiresorptives, is determined by the number of osteoclasts on bone surfaces.

EXPERIMENTAL PROCEDURES

Mice and Materials—Female huRANKL mice, male $RANK^{-/-}$ mice, and their respective wild-type (WT) littermates (C57/129/Black Swiss background) were provided by Amgen Inc. (Thousand Oaks, CA) (31). Recombinant human PTH-(1–34), Aln (Calbiochem, San Diego, CA), and denosumab (DMAb) were generously provided by Amgen Inc.

In Vivo Experiments—HuRANKL mice were ovariectomized (OVX) at 18 weeks of age or sham-operated under ketamine (120 mg/kg)/xylazine (16 mg/kg) anesthesia (Drs. Graub, Bern, and Provet, Lyssach, Switzerland, respectively). Mice had access to mouse chow RM3 (SDS, Betchworth, Surrey, UK) and water *ad libitum* and were exposed to 12 h light, 12 h dark cycle. The day after OVX, mice were assigned to 3 different groups and each pretreated group received either Aln (100 μg/kg, subcutaneous (sc), twice a week), DMAb (10 mg/kg, sc, twice a week), or vehicle (Veh, PBS) for 4 weeks ($n = 6–8$/group). The denosumab dosing regimen was selected for its ability to overcome potential immune responses in these immunocompetent mice toward the fully human denosumab protein. In each pretreated group, mice were then further assigned to PTH (1–34) (80 μg/kg/d, sc) or Veh for 4 weeks ($n = 6–8$/group) while continuing their original treatments. Sham mice ($n = 6$) received Veh for 8 weeks (Fig. 1). Mice received a sc injection of calcein (20 mg/kg, Sigma) at 7 and 2 days before sacrifice, then were sacrificed at week 8, and blood was collected for serum measurements. Lumbar spine and the right femur were excised for micro-computed tomography (micro-CT) analysis and the tibiae processed for histomorphometry. The left femur was excised and frozen at −20 °C for biomechanical testing. The animal protocol for huRANKL mice was approved by the Ethical Committee of the University of Geneva School of Medicine and State of Geneva Veterinarian Office.

Male $RANK^{-/-}$ mice and WT littermates, aged to 7 to 8 weeks of age, were treated by daily sc injection for 14 days with either Veh or with human PTH at 0.4 mg/kg/day ($n = 9–10$/genotype/group). $RANK^{-/-}$ mice, which are severely osteopetrotic and toothless, were maintained on a powdered version of standard mouse chow (Harlan Teklad, Madison, WI). Mice were sacrificed after 2 weeks of treatment and the distal femur

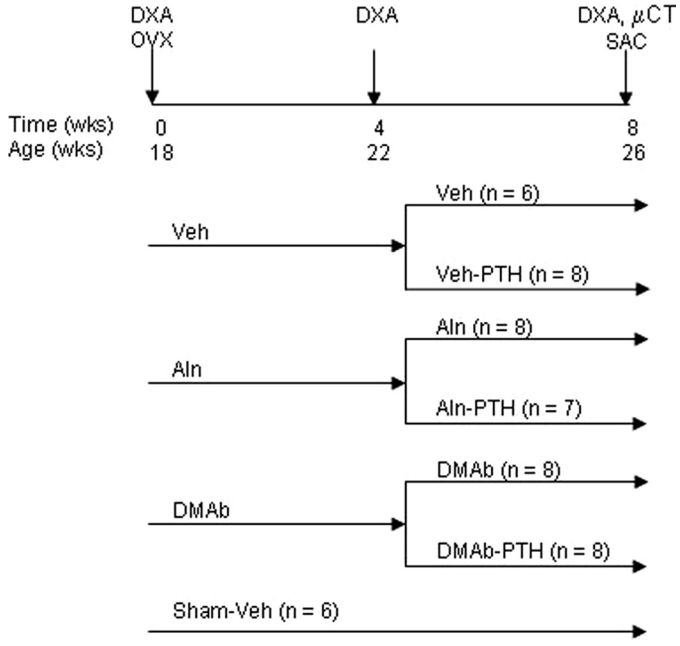

FIGURE 1. **Schematic representation of the experimental design.** huRANKL mice were ovariectomized (*OVX*) or not (*Sham*) at 18 weeks of age and assigned to receive either Veh, Aln, or DMAb treatment. After 4 weeks, mice were further assigned to intermittent PTH (1–34) (80 μg/kg/day) or Veh administration, in addition to Aln, DMAb, or Veh.

was harvested for micro-CT analysis of trabecular volumetric BMD (vBMD). The protocol and procedures for $RANK^{-/-}$ mice were approved by the Institutional Animal Care and Use Committee of Amgen Inc.

Bone Mineral Density and Bone Morphology—In huRANKL mice, total body, spine, and femoral BMD (g/cm^2) was evaluated *in vivo* using dual-energy x-ray absorptiometry (DXA, PIXImus, GE Lunar, Madison, WI). Total body BMD (TB BMD) values were similar between groups at baseline, and data of total body, spine, and femoral BMD are expressed as percent change from baseline. We assessed trabecular and cortical bone architecture at week 8 using micro-CT (μCT40, Scanco Medical AG, Basserdorf, Switzerland), employing a 12 μm isotropic voxel size. Specifically, trabecular bone architecture as well as cortical width (as the mean of the whole section) were evaluated at the 5th lumbar vertebra and distal femoral metaphysis, whereas cortical bone morphology was evaluated at the femoral mid-shaft, as previously described (33, 34).

In $RANK^{-/-}$ mice, vBMD was determined using a desktop micro-CT system (GE eXplore Locus SP Specimen Scanner; GE Healthcare). The whole left femur was scanned and images reconstructed with a 13 μm isotropic voxel size. Contours were drawn to select a trabecular region (10% of femur length) beginning at 30% of the femur length from the distal end in $RANK^{-/-}$ mice and 15% in WT mice. These regions were selected to avoid the distal growth plate, which was wider in $RANK^{-/-}$ mice, and therefore penetrated more deeply into the metaphysis. Cortical regions (10% of femur length) were also selected distal from the femur midpoint for assessment of cortical vBMD, as previously described (22). Because of major differences in BMD between the genotypes, trabecular vBMD was measured without applying thresholds.

Biochemical Determinations—Serum tartrate resistant acid phosphatase form 5b (TRACP5b), osteocalcin, and PTH were measured by ELISA according to manufacturer instructions (IDS Ltd, UK; Biomedical Technologies Inc., Stoughton, MA; and Immunotopics Inc, San Clemente, CA, respectively). In $RANK^{-/-}$ mice, osteocalcin was measured by a Luminex microbead assay (Milipore/Linco, St. Charles, MO).

Biomechanical Testing—The night before mechanical testing, femurs were thawed slowly at 7 °C and then maintained at room temperature. The length of the femur was measured using a digital caliper and the middle of the shaft was determined. The femur was placed in the material testing machine on 2 supports separated by the distance of 9.9 mm, and load was applied to the middle of the shaft, thus creating a 3-point bending test. Between the different steps of preparation, each specimen was kept immersed in physiological solution. The mechanical resistance to failure was tested using a servo-controlled electromechanical system (Instron 1114, Instron Corp., High Wycombe, UK). The cross-head speed for all tests was 2 mm/min and the upper roller contacted the femur at the anterior mid-diaphysis with the load direction perpendicular to the medio-lateral diameter. Both displacement and load were recorded. Maximal load (N) and stiffness (slope of the linear part of the curve representing elastic deformation [N/mm]), were calculated from the load-displacement curves. Ultimate stress (σ_u, MPa) and Young's modulus (E, modulus of elasticity; MPa) were determined by the equations previously described by Turner and Burr (35).

Histology—Tibiae of huRANKL knock-in mice were embedded in methylmethacrylate (Merck), and 5-μm sagittal sections of the proximal third of the tibiae were stained and histomorphometric measurements were performed on the secondary spongiosa, as previously described (36). To measure dynamic indices of bone formation, 8 μm sagittal sections were cut and mounted unstained for evaluation of the calcein labels, as previously described (36). In the DMAb-treated mice, no single- or double-labeled bone surfaces were present in the sections and the different parameters of bone formation were described as "not detectable" in Table 2. These parameters of bone formation included mineralizing surfaces (MS/BS), mineral apposition rate (MAR), and BFR.

Statistical Analysis—For the huRANKL mice, a 2-factor analysis of variance was used to assess the effect of Aln/DMAb and PTH on skeletal morphology. As appropriate, post-hoc testing was performed using Fisher's Protected Least Squares Difference (PLSD). All tests were 2-tailed, with differences considered significant at $p < 0.05$. Data are presented as means ± S.E. of the mean (S.E.), unless otherwise noted.

For the $RANK^{-/-}$ mouse study, 1-way ANOVA followed by Dunnett's test was used to compare differences between Veh-treated WT *versus* $RANK^{-/-}$ knock-out mice, and to compare differences between Veh- and PTH-treated mice within the same genotype. Tests were run using JMP software (SAS Institute, Cary, NC), with $p < 0.05$ used to determine significant differences.

TABLE 1

Effects of Aln, DMAb, Aln plus PTH, or DMAb plus PTH on bone mass and vertebral and femoral microarchitecture in huRANKL mice

In parentheses are the number of mice per group. Conn dens, connectivity density.

	Sham (6)	OVX					
		No PTH			PTH		
		Veh (6)	Aln (8)	DMAb (8)	Veh (6)	Aln (7)	DMAb (8)
BMD change (%, week 8-week 0)							
Total body	−1.0 ± 1.2	−4.1 ± 1.9	2.9 ± 1.0[b]	8.1 ± 1.1[b,c]	1.0 ± 0.8[d]	9.2 ± 1.2[d,f]	5.2 ± 1.9[f,g]
Lumbar spine	−6.8 ± 3.1	−12.5 ± 5.6	7.6 ± 4.0[b]	7.8 ± 4.5[b]	−12.1 ± 2.5	11.6 ± 4.3[f]	6.3 ± 4.1[f]
Femoral shaft	−3.2 ± 1.3	−1.6 ± 2.8	3.4 ± 1.9	5.5 ± 1.8[b]	−6.1 ± 1.1	4.1 ± 2.0[f]	4.8 ± 3.6[f]
Vertebral trabecular bone							
BV/TV (%)	21.8 ± 1.6	15.7 ± 1.3[a]	22.6 ± 0.7[b]	23.7 ± 1.6[b]	18.7 ± 1.2	28.8 ± 1.8[d,f]	24.1 ± 1.9[f,g]
Tb N (/mm)	3.4 ± 0.1	2.9 ± 0.2[a]	3.6 ± 0.2[b]	3.7 ± 0.2[b]	3.0 ± 0.1	3.6 ± 0.1[f]	3.6 ± 0.1[f]
Tb Th (μm)	62.5 ± 2.9	55.2 ± 1.7[a]	59.0 ± 0.9	62.5 ± 2.[b]	59.0 ± 0.8	69.3 ± 1.5[d,f]	62.9 ± 2.5[g]
Conn dens (mm^{-3})	84.1 ± 4.1	89.0 ± 9.4	85.2 ± 6.4	97.2 ± 6.5	112.6 ± 15.9	81.3 ± 5.4[f]	98.2 ± 9.7
Cortical width (μm)	95.3 ± 1.7	83.3 ± 2.1[a]	100.3 ± 2.1[b]	123.4 ± 5.8[b,c]	92.1 ± 2.0	114.0 ± 3.5[d,f]	114.5 ± 6.3[f]
Distal femur trabecular bone							
BV/TV (%)	5.0 ± 0.8	1.3 ± 0.3[a]	4.4 ± 0.5	8.5 ± 1.4[b,c]	2.3 ± 0.4	8.6 ± 1.4[d,f]	7.0 ± 1.3[f]
Tb N (/mm)	2.7 ± 0.2	1.6 ± 0.1[a]	2.8 ± 0.1[b]	3.9 ± 0.4[b,c]	1.9 ± 0.2	3.6 ± 0.3[d,f]	3.6 ± 0.4[f]
Tb Th (μm)	42.4 ± 1.9	37.4 ± 2.3[a]	38.5 ± 0.9	43.2 ± 1.3[b,c]	42.1 ± 0.9[d]	45.3 ± 0.8[d]	40.8 ± 1.5[g]
Conn dens (mm^{-3})	25.1 ± 6.6	2.5 ± 0.7	30.6 ± 4.6	66.8 ± 14.3[b,c]	7.4 ± 1.6	72.4 ± 19.2[d,f]	52.0 ± 12.3[f]
Cortical width (μm)	133.4 ± 3.6	108.7 ± 5.4[a]	122.3 ± 3.3[b]	131.8 ± 5.4[b]	117.4 ± 3.4	126.2 ± 3.2	129.4 ± 4.7[f]
Femoral cortical bone							
Cross sectional area (mm^2)	0.272 ± 0.005	0.260 ± 0.006	0.279 ± 0.008	0.283 ± 0.014	0.279 ± 0.007	0.286 ± 0.006	0.272 ± 0.007
Bone area (mm^2)	0.164 ± 0.002	0.140 ± 0.002[a]	0.160 ± 0.005[b]	0.153 ± 0.003[b]	0.151 ± 0.003[d]	0.167 ± 0.004[f]	0.157 ± 0.003
Medullary area (mm^2)	0.108 ± 0.003	0.120 ± 0.005	0.119 ± 0.005	0.130 ± 0.013	0.128 ± 0.005	0.119 ± 0.003	0.114 ± 0.005
Cortical width (μm)	274 ± 1	239 ± 4[a]	262 ± 7[b]	251 ± 5	246 ± 4	267 ± 6[f]	262 ± 5[f]

[a] $p < 0.05$ compared with sham.
[b] $p < 0.05$ compared with OVX Veh.
[c] $p < 0.05$ compared with OVX Aln.
[d] $p < 0.05$ compared with non-PTH in the same pretreatment group.
[f] $p < 0.05$ compared with OVX Veh-PTH.
[g] $p < 0.05$ compared with OVX Aln-PTH.

RESULTS

Effects of Aln, DMAb, and Combination with PTH on Bone Mass and Microarchitecture in OVX huRANKL Mice—In OVX huRANKL mice, Aln and DMAb both prevented bone loss at the lumbar spine and femur, although DMAb caused a significantly greater increase in TB BMD compared with Aln after 4 and 8 weeks (Table 1 and Fig. 2*A*). OVX decreased cancellous bone volume fraction (BV/TV), trabecular number (Tb N) and thickness (Tb Th), and cortical width at the distal femur and vertebrae, as well as cortical width at the midshaft femur ($p <$ 0.05 compared with sham). Aln and DMAb maintained bone microstructure at these skeletal sites (Table 1 and Fig. 2, *B–E*), but DMAb caused significantly greater increases than Aln in microarchitectural parameters at the distal femur and vertebral cortical thickness (Table 1 and Fig. 2*B*).

Daily PTH administered between 4 and 8 weeks post-OVX improved TB BMD compared with OVX, but did not impact BMD at the lumbar spine or femoral shaft. In combination with Aln, PTH markedly improved BMD at all sites and was significantly better than Aln alone. In contrast, PTH combined with DMAb did not further improve TB BMD compared with DMAb alone (Table 1 and Fig. 2*A*). Compared with Veh, PTH alone significantly increased Tb Th at the distal femur and bone area at the femoral midshaft (Table 1). PTH in combination with Aln, compared with Aln alone, significantly increased cancellous bone parameters in distal femur and vertebrae, including BV/TV and Tb Th (Table 1 and Fig. 2*B*). The PTH and Aln combination also improved cancellous and cortical bone parameters compared with PTH alone, confirming that the 2 treatments exerted additive effects (Table 1 and Fig. 2*B*). In contrast, PTH exerted no additional effects on microarchitecture when combined with DMAb (Table 1 and Fig. 2, *B–E*).

Effects of Aln, DMAb, and Combination with PTH on Bone Strength in OVX huRANKL Mice—Treatment effects on bone strength were further evaluated at the midshaft femur by 3-point bending tests. PTH was most effective at improving the moment of inertia and the cortical structural properties, such as stiffness, compared with Veh (supplemental Table S1). Aln and DMAb both prevented the decrease in Young's modulus but did not improve cortical stiffness compared with Veh (Fig. 2*D* and supplemental Table S1). The effects of PTH on the structural properties (maximal load and stiffness) were maintained in combination with Aln, although they were not better than PTH alone. In DMAb-treated mice, PTH showed a non-significant trend to improve femur strength compared DMAb alone (Fig. 2*D* and supplemental Table S1), suggesting that PTH effects on bone-modeling surfaces could be maintained (see below, $RANK^{-/-}$ mice).

Biochemical Markers of Bone Turnover and Their Relationship to Bone Mass and Structure in huRANKL Mice—OVX increased TRACP5b and transiently increased osteocalcin compared with baseline. These changes were prevented by Aln, however DMAb further decreased markers of bone turnover and there was a significant and persistent increase of serum PTH in DMAb-treated mice (Fig. 3*A*). We next correlated TRACP5b values at sacrifice with parameters of bone mass and structure in OVX Veh-, Aln-, and DMAb-treated mice. TB BMD, vertebral BV/TV, and cortical thickness, as well as serum PTH levels were all negatively and significantly correlated with post-treatment TRACP5b levels (Fig. 3*B*). This indicates that the greater the

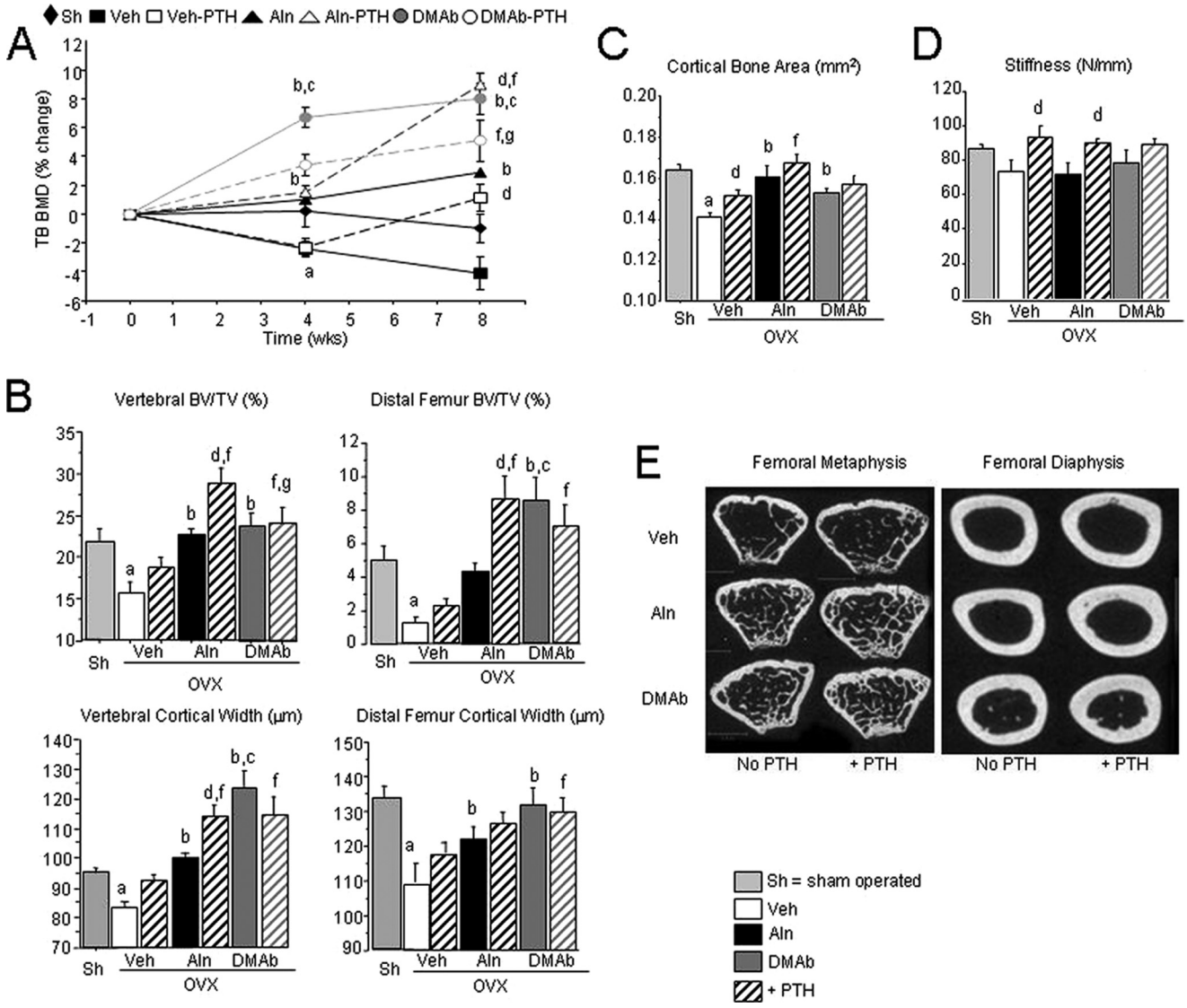

FIGURE 2. **BMD, bone microarchitecture, and strength in OVX huRANKL mice treated with Aln or DMAb, with or without PTH.** *A*, effects of the different noted therapies on TB BMD. Data are expressed as the percentage change from baseline (0 week), DXA (± S.E.). Vertebral and femoral cancellous (*B*) and cortical (*C*) microarchitecture at the midshaft femur, and femoral stiffness (*D*) in OVX huRANKL mice treated with Aln or DMAb, with or without PTH, for 8 weeks post-OVX. *E*, two dimensional micro-CT representative images of the femoral metaphysis and diaphysis for each treatment group. *a*, $p < 0.05$ compared with Sham; *b*, $p < 0.05$ compared with OVX Veh; *c*, $p < 0.05$ compared with OVX Aln; *d*, $p < 0.05$ compared with non-PTH in the same pretreatment group; *e*, $p < 0.05$ compared with baseline; *f*, $p < 0.05$ compared with OVX Veh-PTH; *g*, $p < 0.05$ compared with OVX Aln-PTH.

suppression of osteoclasts and bone resorption, the better the bone mass and structure in a monotherapy setting.

The addition of intermittent PTH increased osteocalcin in all groups compared with the other non-PTH treatment groups, reaching significance in the DMAb-PTH *versus* DMAb group. However, mean osteocalcin levels remained significantly lower in DMAb-PTH than in the Veh-PTH or Aln-PTH groups.

Treatment Effects on Bone Remodeling Indices in huRANKL Mice—As evaluated by histomorphometry of cancellous bone at the proximal tibia metaphysis, osteoclast surface (OcS/BS), and osteoclast number (OcN) were decreased with DMAb and increased with Aln (Table 2). The addition of PTH resulted in a significant increase in OcS/BS and OcN in DMAb-treated mice, although these values remained lower than in the Aln-treated group. Bone forming indices also differed between antiresorptives. Aln decreased MS/BS and BFR compared with Veh, but had no significant effects on MAR (Table 2). DMAb suppressed all bone forming indices, as shown by the lack of single- or double-labeled surfaces. Intermittent PTH alone clearly increased bone-forming indices, as well as in combination with Aln or DMAb. In particular, MAR was similar in the DMAb-PTH and Aln-PTH groups, and only 25–35% lower compared with PTH alone. In contrast, PTH effects on BFR were more markedly affected by the antiresorptives, as it remained 40% lower in presence of Aln, and 75% lower in presence of DMAb, compared with PTH alone (Table 2 and Fig. 4*A*). BFR however was not correlated to osteoclast surfaces/numbers in the PTH-treated groups (Fig. 4*B*), suggesting that osteoclasts were not the most important determinants of the bone-forming response to PTH.

However, PTH had induced the appearance of some osteoclasts in DMAb-treated mice, which might have contributed

to the PTH anabolism they exhibited by histomorphometry and by serum osteocalcin. We therefore examined the potential for PTH anabolism in RANK$^{-/-}$ mice, which are virtually devoid of osteoclasts even when stimulated with PTH (31).

Effects of Intermittent PTH in RANK$^{-/-}$ Mice—For this purpose we treated osteoclast-less RANK$^{-/-}$ mice and WT controls with high-dose PTH (400 μg/kg/d) for 2 weeks. PTH significantly increased osteocalcin and TRACP5b levels in WT mice (Fig. 5, *A* and *B*). In RANK$^{-/-}$ mice, TRACP5b levels were 91% lower than in WT mice and did not change with PTH. Nevertheless, PTH increased serum osteocalcin in RANK$^{-/-}$ mice similarly to WT, indicating that increased osteocalcin induced by PTH can occur independently of osteoclasts or bone resorption. Distal femur trabecular vBMD was markedly increased in Veh-treated RANK$^{-/-}$ mice compared with Veh-treated WT controls (Fig. 5*C*). Two weeks of intermittent PTH increased trabecular vBMD by 66% in WT and by 15% in RANK$^{-/-}$ mice compared with Veh. PTH also significantly increased cortical vBMD in the femoral midshaft of RANK$^{-/-}$ mice, from 900.0 mg/cm^3 (Veh controls) to 981.5 mg/cm^3 ($p < 0.05$). In contrast, PTH caused an expected and modest reduction in cortical vBMD in WT mice, from 1086.8 mg/cm^3 (Veh) to 1061.7 mg/cm^3 (non-significant). Representative micro-CT images of trabecular bone from the distal femoral metaphysis of each group are shown in Fig. 5*D*.

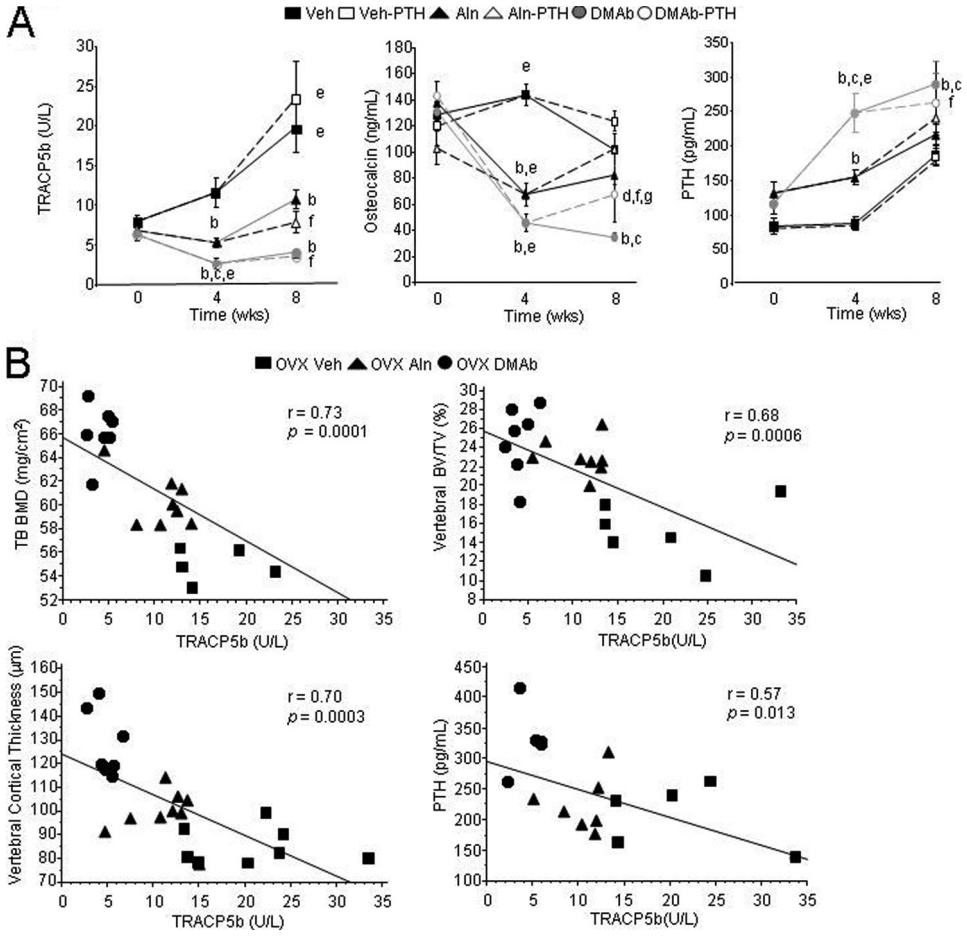

FIGURE 3. **Bone serum markers of remodeling and correlation to bone mass and structure in huRANKL mice treated with Aln or DMAb, with or without PTH, 8 weeks post-OVX.** *A*, serum TRACP5b, osteocalcin, and PTH were measured at time 0, week 4, and week 8 (sacrifice). *B*, correlation between TRACP5b levels (marker of bone turnover) and bone mass, architecture, and PTH. All parameters were measured 8 weeks post-OVX in OVX Veh-, Aln-, and DMAb-treated huRANKL mice. *a*, $p < 0.05$ compared with Sham; *b*, $p < 0.05$ compared with OVX Veh; *c*, $p < 0.05$ compared with OVX Aln; *d*, $p < 0.05$ compared with non-PTH in the same pretreatment group; *e*, $p < 0.05$ compared with baseline; *f*, $p < 0.05$ compared with OVX Veh-PTH; *g*, $p < 0.05$ compared with OVX Aln-PTH.

DISCUSSION

In this study, we examined the role of osteoclasts and bone remodeling in the bone anabolic response to intermittent PTH. More specifically, we evaluated whether PTH

TABLE 2

Bone remodeling indices on cancellous bone surfaces in OVX huRANKL mice treated with Aln, DMAb, Aln plus PTH, or DMAb plus PTH

In parenthesis are the number of mice per group.

	Sham (6)	OVX					
		No PTH			PTH		
		Veh (6)	Aln (8)	DMAb (6)	Veh (3)	Aln (5)	DMAb (5)
Single-labeled bone surface/BS (%)	0.928 ± 0.074	1.580 ± 0.119[a]	1.150 ± 0.111[b]	n.d.	0.653 ± 0.080[d]	0.810 ± 0.118[d,f]	0.497 ± 0.149[d,g]
Double-labeled bone surface/BS (%)	0.652 ± 0.088	0.751 ± 0.297	0.069 ± 0.012[b]	n.d.	1.117 ± 0.117[d]	0.591 ± 30.050[d,f]	0.338 ± 0.206[d,f]
MS/BS (%)	22.78 ± 2.06	22.84 ± 2.82	12.16 ± 0.9[b]	n.d.	31.18 ± 1.02[d]	26.24 ± 0.83[d]	11.51 ± 4.57[d,f,g]
MAR (μm/day)	1.71 ± 0.17	1.50 ± 0.07	1.30 ± 0.17	n.d.	1.99 ± 0.03	1.50 ± 0.24	1.31 ± 0.20[d,f]
BFR/BS (μm^3/μm^2/day)	0.38 ± 0.05	0.35 ± 0.06	0.16 ± 0.03[b]	n.d.	0.62 ± 0.01[d]	0.39 ± 0.06[d,f]	0.17 ± 0.08[d,f,g]
OcS/BS (%)	8.87 ± 1.28	10.29 ± 0.92	16.11 ± 1.58[b]	0.78 ± 0.10[b,c]	8.37 ± 0.29	13.056 ± 2.05[f]	5.12 ± 1.29[d,g]
OcN (/mm)	50.7 ± 6.2	29.2 ± 6.7	134.4 ± 13.2[b]	8.1 ± 1.3[c]	35.0 ± 3.1	91.4 ± 17.8[d,f]	39.8 ± 9.7[d,g]

[a] $p < 0.05$ compared with sham.
[b] $p < 0.05$ compared with OVX Veh.
[c] $p < 0.05$ compared with OVX Aln.
[d] $p < 0.05$ compared with non-PTH in the same pretreatment group.
[f] $p < 0.05$ compared with OVX Veh-PTH.
[g] $p < 0.05$ compared with OVX-Veh-Aln.
n.d., not detectable.

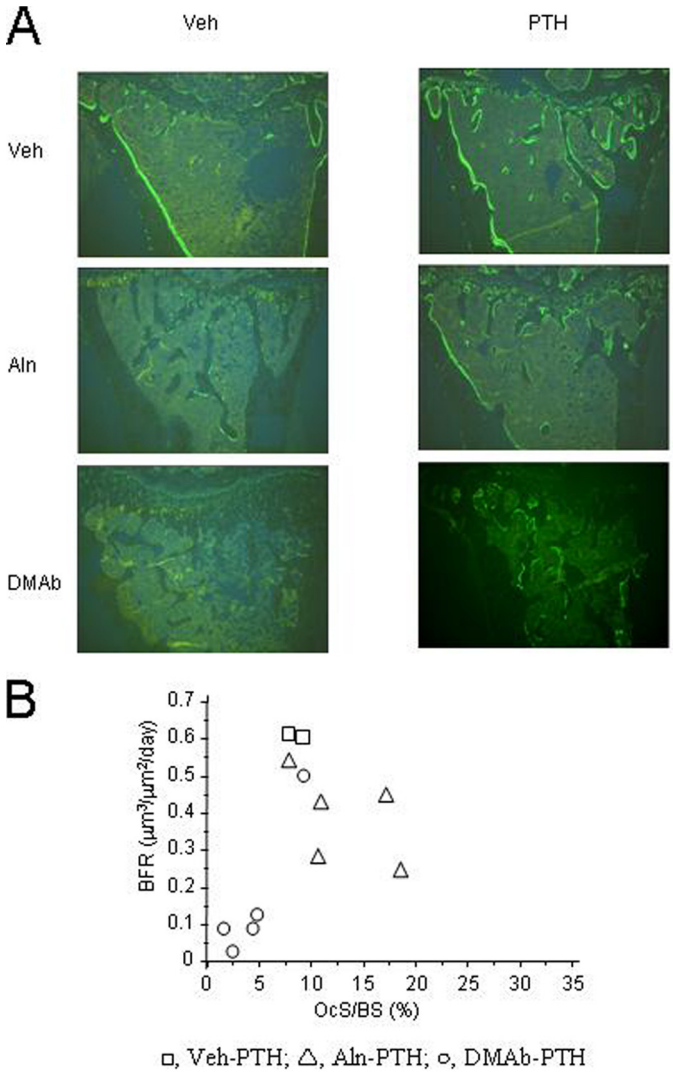

FIGURE 4. **Tibial histology for huRANKL mice.** *A*, representative histologic images (sagittal section) of tibial cancellous bone of each treatment group after treatment with Aln or DMAb, with or without PTH, 8 weeks post-OVX. *B*, correlation between cancellous OcS/BS *versus* BFR for PTH-treated animals.

could exert additive effects on bone mass in the model of the OVX huRANKL mouse treated with the potent osteoclast inhibitor DMAb. At the doses tested in this study, DMAb caused greater suppression of bone turnover than Aln, resulting in further improvements in BMD and cancellous microarchitecture. In turn, intermittent PTH exerted additive effects with Aln, but not with DMAb.

DMAb and Aln exert their antiresorptive action through different mechanisms. DMAb selectively binds to RANKL and inhibits osteoclast-mediated bone resorption, osteoclast maturation, and survival, while Aln binds to the mineralized bone matrix and decreases osteoclast activity, without necessarily reducing the number of osteoclasts (37–39). Treatment of OVX huRANKL mice with DMAb alone was associated with a marked reduction of osteoclast surfaces and with histological parameters of bone formation that were barely detectable. The latter finding indicates that remodeling is the predominant physiological form of bone turnover in these mice at this age, and that remodeling was markedly suppressed by DMAb. In contrast to the effects of DMAb, Aln monotherapy resulted in a paradoxic and significant increase in osteoclast surfaces and an expected reduction in bone formation parameters that was consistent with the diminution of bone remodeling. Histologic and biochemical remodeling parameters were more suppressed with DMAb than with Aln, and BMD increases were generally greater with DMAb than with Aln. These findings are consistent with previous head-to-head comparisons in human and non-human primates treated with these agents (40, 41).

In huRANKL mice, administration of intermittent PTH increased BMD, cortical bone area, and stiffness, in addition to its effects on BFR at cancellous bone surfaces, compared with OVX. When PTH was added to Aln, it still increased bone-forming indices and exerted clear additive effects on BMD and microarchitecture, consistent with previous data (27, 28). Some clinical trials have reported that in patients treated with Aln, before as well as during exposure to PTH, the combined therapy was superior to Aln alone (42, 43). However, it has not been demonstrated that the BMD response to PTH plus antiresorptives is superior to PTH alone in humans. When combined with DMAb, PTH was able to somewhat reactivate osteoclastogenesis, as shown by an increase of osteoclast numbers on cancellous bone. PTH also increased bone-forming indices in the presence of DMAb, indicating that the suppression of bone turnover with DMAb was at least partially reversible, even when DMAb treatment was continued at a dose level that greatly exceeds those used clinically. Most importantly, PTH-stimulated MAR reached similar levels in presence of DMAb and Aln, despite large differences in the number of osteoclasts, indicating that stimulation of osteoblast activity is largely independent of osteoclast number and activity. However, MS/BS and BFR remained markedly reduced when PTH was administered with DMAb compared with intermittent PTH alone, indicating that a critical reduction in osteoclast numbers, and thereby of remodeling surfaces, may compromise the extent of PTH anabolic effects, which could explain why PTH and DMAb failed to exert additional effects on bone mass and microarchitecture.

There are other potential explanations for the lack of an additive BMD effect when PTH was added to DMAb-treated animals. The 4-week period of PTH co-administration with DMAb might not have been sufficient to observe additive effects on BMD. In an aged OVX rat study, the additive effect of PTH plus OPG on vertebral BMD compared with PTH alone was not apparent until 3 months after their co-administration (28). However, 4 weeks was adequate to observe additive effects of PTH plus Aln on BMD under the conditions of the current study. Another possibility relates to the DMAb dosing regimen (10 mg/kg, twice weekly), which greatly exceeds the dose used clinically for bone loss (1 mg/kg, twice yearly). This DMAb dosing regimen, which was used to ensure adequate drug exposure in the face of potential immune responses to this fully human protein, might limit the ability of these findings to predict clinical outcomes in humans. Finally, animals pre-treated with DMAb had higher BMD than those pretreated with Aln at the time PTH was introduced, which could limit the former group potential for further BMD increments with PTH. Consistent with this notion, PTH was able to increase BMD much

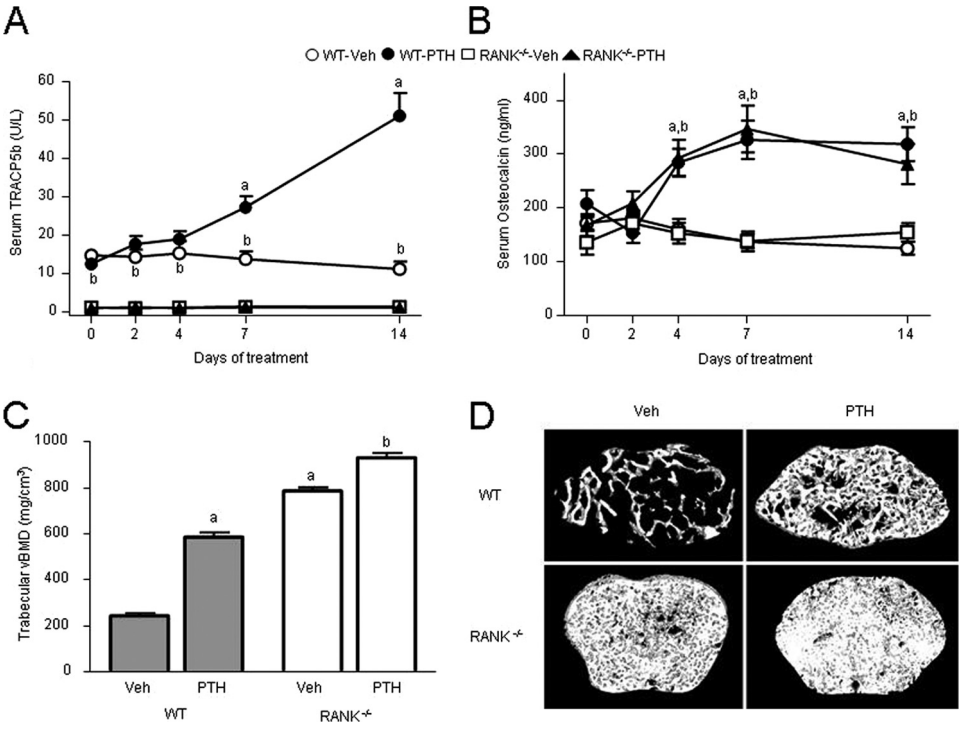

FIGURE 5. **Effects of 2 weeks of intermittent PTH treatment on serum TRACP5b, osteocalcin, and trabecular BMD in WT and RANK$^{-/-}$ mice.** *A*, serum TRACP in WT and RANK$^{-/-}$ mice in response to PTH. *B*, serum osteocalcin in PTH-treated WT and RANK$^{-/-}$ mice. *C*, effects of PTH on trabecular vBMD in the distal femur metaphysis of WT and RANK$^{-/-}$ mice. *D*, representative micro-CT images of the distal femur metaphysis of WT and RANK$^{-/-}$ mice treated with Veh or with intermittent PTH. Selected images represent the median trabecular bone volume fraction value from each group. *a*, $p < 0.05$ compared with Veh-treated WT; *b*, $p < 0.05$ compared with Veh-treated RANK$^{-/-}$.

more in WT mice compared with osteopetrotic RANK$^{-/-}$ mice. Nonetheless, the overall data are consistent with the hypothesis that trabecular bone remodeling is an important attribute of PTH anabolism in huRANKL mice.

If remodeling is indeed important for PTH anabolism, it is important to understand why, under certain conditions, PTH is capable of robustly increasing BMD in mice or rats co-treated with potent antiresorptives such as Aln (28, 29, 30) or OPG (28, 30). This is a particularly important question because the additive effects of PTH and Aln on vertebral BMD in rodents stands in contrast to the blunted vertebral BMD response to PTH plus Aln *versus* PTH alone in human studies (9, 10). One hypothesis is that mice and rats have a greater capacity than humans for PTH stimulation of modeling-based bone formation, which occurs in the absence of prior osteoclast activation.

The extent to which PTH can increase BMD in mice via pure modeling-based bone formation was examined by administering PTH to RANK$^{-/-}$ mice, which are devoid of osteoclasts and are therefore incapable of true bone remodeling (32). A short (2-week) duration was chosen to minimize handling and stress to the severely osteopetrotic and toothless RANK$^{-/-}$ mice. A high dose of PTH was used to produce a sufficiently robust BMD response of WT mice to PTH, over this brief treatment period, to determine whether or not RANK$^{-/-}$ mice were truly resistant to PTH. It was not possible to perform reliable histomorphometry on trabecular surfaces in RANK$^{-/-}$ mice, due to their lack of marrow space and absence of clearly defined trabecular surfaces (32). However, it was previously shown that the local injection of an even higher concentration (~1,400 μg/kg/day) of parathyroid hormone-related protein (PTHrP), which activates the same receptor as PTH, was unable to induce the appearance of any osteoclasts in the calvaria of RANK$^{-/-}$ mice (32). In the current study, short-term administration of high-dose PTH (400 μg/kg/day) resulted in an increase of serum osteocalcin that was similar to WT mice, indicating that both genotypes could exhibit bone-forming responses to PTH.

PTH-mediated increases in serum osteocalcin in aged OVX rats were previously shown to be unaffected by co-administration of recombinant OPG (29), suggesting that this phenomenon is not restricted to young osteopetrotic mice and does not require high doses of PTH. Also, PTH significantly increased trabecular vBMD in RANK$^{-/-}$ mice, even though their baseline trabecular vBMD was already extremely high. This high bone mass phenotype probably explains why the BMD response to PTH in RANK$^{-/-}$ mice was somewhat lower than the response observed in WT controls, which had much more marrow space available for new bone formation. The osteocalcin and BMD responses to PTH in RANK$^{-/-}$ mice occurred despite very low basal levels of serum TRACP5b, and despite a complete lack of response of this osteoclast marker to PTH. It is also interesting to note that PTH also increased cortical vBMD in RANK$^{-/-}$ mice, but not in WT mice. Increased cortical BMD is not typically observed with PTH administration, primarily due to increases in osteoclast-mediated cortical porosity (44). Hence several lines of evidence indicate that bone formation could be stimulated in RANK$^{-/-}$ mice in the absence of basal or stimulated bone resorption. The fact that PTH increased BMD in RANK$^{-/-}$ mice but not in DMAb-treated huRANKL mice could relate to the higher dose of PTH.

Erben showed that in young rats, most of the cancellous bone forming sites in the untreated condition were modeling-based (4). Compared with young rats or mice, the extent of modeling-based bone formation in the untreated adult human osteoporotic skeleton is likely to be much lower (45). The extent to which PTH can stimulate modeling-based bone formation in this population is unclear. Current evidence indicates that this extent is very low in the steady-state situation after long-term PTH therapy (5), but could be higher during the earlier phase of treatment (6). Based on these observations and the current results, it seems reasonable to hypothesize that the net effects of PTH on trabecular

BMD in postmenopausal women receiving DMAb would be greatest in the early period of concomitant therapy, prior to the refilling of remodeling space (*i.e.* short-lived). Over the long term, the overall BMD response to PTH in DMAb-treated subjects might be determined primarily by the capacity of PTH to promote trabecular modeling-based bone formation, and hence remain quite modest. At cortical sites, antiresorptive co-therapy with Aln does not appear to significantly blunt PTH-mediated BMD increases (9, 10). This outcome might reflect the potential for Aln to reduce cortical porosity and remodeling-based cortical bone formation, which could have offsetting effects on cortical BMD in that population. Similarly, DMAb significantly reduced cortical bone remodeling and cortical porosity in adult OVX cynomolgus monkeys (46) and RANKL inhibition by OPG reduced cortical porosity in mice with constitutively active PTH receptors (47). The ability of PTH to increase cortical vBMD in $RANK^{-/-}$ mice, in which bone resorption was at undetectable levels, suggests that intermittent PTH therapy might have positive effects on cortical BMD in patients co-treated with DMAb.

In summary, DMAb reduced bone remodeling and increased BMD in OVX huRANKL mice to a greater extent than Aln at the doses tested. While BMD tended to be increased by the addition of PTH treatment in animals pretreated with Aln, this additive effect was not apparent in mice pre-treated with DMAb. These results are consistent with the hypothesis that the capacity for bone remodeling, and the availability of remodeling space, are generally important attributes of PTH anabolism. Whether this remodeling capacity is advantageous in terms of the overall potential for BMD gains in response to PTH is unclear, as BMD in animals treated with Aln plus PTH was generally similar to BMD in animals treated with DMAb alone, in which remodeling space was minimal. The fact that PTH increased bone mass in $RANK^{-/-}$ mice, which are devoid of osteoclasts and which showed no evidence of bone resorption with PTH administration, demonstrates that mice also have a significant capacity for PTH-stimulated modeling-based bone formation. The balance of modeling- and remodeling-based bone formation might ultimately dictate skeletal responsiveness to PTH and the ability of PTH to increase bone mass in the presence of antiresorptive co-therapy. The huRANKL mouse study also provides the first evidence that PTH can significantly increase histologic parameters of bone resorption and bone formation despite the co-administration of DMAb. This observation suggests that DMAb might still permit the local activation of bone remodeling at the tissue level under certain stimulated conditions, even when systemic turnover appears to remain very low. Future studies will examine whether such local stimulation of remodeling might lead to increased BMD with PTH treatment after longer periods of co-treatment with DMAb. From these observations we conclude that antiresorptives did not preclude PTH anabolic effects on the skeleton and that neither bone resorption nor osteoclasts were strictly necessary for PTH-induced bone formation. However, a reduction in osteoclast number and/or surface, by limiting the extent of the remodeling space, will restrict the actions of PTH to the modeling space, which may then require higher doses and/or longer periods of administration to be effective at increasing bone mass.

Acknowledgments—We thank Fanny Cavat and Madeleine Lachize of Geneva, and Frank Asuncion, Denise Dwyer, and Sean Morony of Amgen Inc. for their skillful technical expertise. Erica Rockabrand, PhD of Amgen Inc. provided assistance with editing and formatting.

REFERENCES

1. Cosman, F. (2008) *Curr. Opin. Endocrinol. Diabetes Obes.* **15,** 495–501
2. Girotra, M., Rubin, M. R., and Bilezikian, J. P. (2006) *Rev. Endocr. Metab. Disord.* **7,** 113–121
3. Hodsman, A. B., and Steer, B. M. (1993) *Bone* **14,** 523–527
4. Erben, R. G. (1996) *Anat. Rec.* **246,** 39–46
5. Ma, Y. L., Zeng, Q., Donley, D. W., Ste-Marie, L. G., Gallagher, J. C., Dalsky, G. P., Marcus, R., and Eriksen, E. F. (2006) *J. Bone Miner. Res.* **21,** 855–864
6. Lindsay, R., Cosman, F., Zhou, H., Bostrom, M. P., Shen, V. W., Cruz, J. D., Nieves, J. W., and Dempster, D. W. (2006) *J. Bone Miner. Res.* **21,** 366–373
7. Sato, M., Westmore, M., Ma, Y. L., Schmidt, A., Zeng, Q. Q., Glass, E. V., Vahle, J., Brommage, R., Jerome, C. P., and Turner, C. H. (2004) *J. Bone Miner. Res.* **19,** 623–629
8. Dempster, D. W., Parisien, M., Silverberg, S. J., Liang, X. G., Schnitzer, M., Shen, V., Shane, E., Kimmel, D. B., Recker, R., Lindsay, R., and Bilezikian, J. P. (1999) *J. Clin. Endocrinol. Metab.* **84,** 1562–1566
9. Black, D. M., Greenspan, S. L., Ensrud, K. E., Palermo, L., McGowan, J. A., Lang, T. F., Garnero, P., Bouxsein, M. L., Bilezikian, J. P., and Rosen, C. J. (2003) *N. Engl. J. Med.* **349,** 1207–1215
10. Finkelstein, J. S., Hayes, A., Hunzelman, J. L., Wyland, J. J., Lee, H., and Neer, R. M. (2003) *N. Engl. J. Med.* **349,** 1216–1226
11. Finkelstein, J. S., Leder, B. Z., Burnett, S. M., Wyland, J. J., Lee, H., de la Paz, A. V., Gibson, K., and Neer, R. M. (2006) *J. Clin. Endocrinol. Metab.* **91,** 2882–2887
12. Martin, T. J., Quinn, J. M., Gillespie, M. T., Ng, K. W., Karsdal, M. A., and Sims, N. A. (2006) *Ann. N.Y. Acad. Sci.* **1068,** 458–470
13. Henriksen, K., Neutzsky-Wulff, A. V., Bonewald, L. F., and Karsdal, M. A. (2009) *Bone* **44,** 1026–1033
14. Martin, T. J., and Sims, N. A. (2005) *Trends Mol. Med.* **11,** 76–81
15. Zhao, C., Irie, N., Takada, Y., Shimoda, K., Miyamoto, T., Nishiwaki, T., Suda, T., and Matsuo, K. (2006) *Cell Metab.* **4,** 111–121
16. Allan, E. H., Häusler, K. D., Wei, T., Gooi, J. H., Quinn, J. M., Crimeen-Irwin, B., Pompolo, S., Sims, N. A., Gillespie, M. T., Onyia, J. E., and Martin, T. J. (2008) *J. Bone Miner. Res.* **23,** 1170–1181
17. Pierroz, D. D., Rufo, A., Bianchi, E. N., Glatt, V., Capulli, M., Rucci, N., Cavat, F., Rizzoli, R., Teti, A., Bouxsein, M. L., and Ferrari, S. L. (2009) *J. Bone Miner. Res.* **24,** 775–784
18. Chavassieux, P., Asser Karsdal, M., Segovia-Silvestre, T., Neutzsky-Wulff, A. V., Chapurlat, R., Boivin, G., and Delmas, P. D. (2008) *J. Bone Miner. Res.* **23,** 1076–1083
19. Dougall, W. C., Glaccum, M., Charrier, K., Rohrbach, K., Brasel, K., De Smedt, T., Daro, E., Smith, J., Tometsko, M. E., Maliszewski, C. R., Armstrong, A., Shen, V., Bain, S., Cosman, D., Anderson, D., Morrissey, P. J., Peschon, J. J., and Schuh, J. (1999) *Genes Dev.* **13,** 2412–2424
20. Kong, Y. Y., Yoshida, H., Sarosi, I., Tan, H. L., Timms, E., Capparelli, C., Morony, S., Oliveira-dos-Santos, A. J., Van, G., Itie, A., Khoo, W., Wakeham, A., Dunstan, C. R., Lacey, D. L., Mak, T. W., Boyle, W. J., and Penninger, J. M. (1999) *Nature* **397,** 315–323
21. Min, H., Morony, S., Sarosi, I., Dunstan, C. R., Capparelli, C., Scully, S., Van, G., Kaufman, S., Kostenuik, P. J., Lacey, D. L., Boyle, W. J., and Simonet, W. S. (2000) *J. Exp. Med.* **192,** 463–474
22. Ominsky, M. S., Stolina, M., Li, X., Corbin, T. J., Asuncion, F. J., Barrero, M., Niu, Q. T., Dwyer, D., Adamu, S., Warmington, K. S., Grisanti, M., Tan, H. L., Ke, H. Z., Simonet, W. S., and Kostenuik, P. J. (2009) *J. Bone Miner. Res.* **24,** 1234–1246
23. Simonet, W. S., Lacey, D. L., Dunstan, C. R., Kelley, M., Chang, M. S., Lüthy, R., Nguyen, H. Q., Wooden, S., Bennett, L., Boone, T., Shimamoto, G., DeRose, M., Elliott, R., Colombero, A., Tan, H. L., Trail, G., Sullivan, J., Davy, E., Bucay, N., Renshaw-Gegg, L., Hughes, T. M., Hill, D., Pattison, W., Campbell, P., Sander, S., Van, G., Tarpley, J., Derby, P., Lee, R., and

Boyle, W. J. (1997) *Cell* **89,** 309–319
24. Bucay, N., Sarosi, I., Dunstan, C. R., Morony, S., Tarpley, J., Capparelli, C., Scully, S., Tan, H. L., Xu, W., Lacey, D. L., Boyle, W. J., and Simonet, W. S. (1998) *Genes Dev.* **12,** 1260–1268
25. Hsu, H., Lacey, D. L., Dunstan, C. R., Solovyev, I., Colombero, A., Timms, E., Tan, H. L., Elliott, G., Kelley, M. J., Sarosi, I., Wang, L., Xia, X. Z., Elliott, R., Chiu, L., Black, T., Scully, S., Capparelli, C., Morony, S., Shimamoto, G., Bass, M. B., and Boyle, W. J. (1999) *Proc. Natl. Acad. Sci. U.S.A.* **96,** 3540–3545
26. Kostenuik, P. J., Capparelli, C., Morony, S., Adamu, S., Shimamoto, G., Shen, V., Lacey, D. L., and Dunstan, C. R. (2001) *Endocrinology* **142,** 4295–4304
27. Samadfam, R., Xia, Q., and Goltzman, D. (2007) *Endocrinology* **148,** 2778–2787
28. Samadfam, R., Xia, Q., and Goltzman, D. (2007) *J. Bone Miner. Res.* **22,** 55–63
29. Kostenuik, P. J. (2005) *Curr. Opin. Pharmacol.* **5,** 618–625
30. Johnston, S., Andrews, S., Shen, V., Cosman, F., Lindsay, R., Dempster, D. W., and Iida-Klein, A. (2007) *Endocrinology* **148,** 4466–4474
31. Kostenuik, P. J., Nguyen, H. Q., McCabe, J., Warmington, K. S., Kurahara, C., Sun, N., Chen, C., Li, L., Cattley, R. C., Van, G., Scully, S., Elliott, R., Grisanti, M., Morony, S., Tan, H. L., Asuncion, F., Li, X., Ominsky, M. S., Stolina, M., Dwyer, D., Dougall, W. C., Hawkins, N., Boyle, W. J., Simonet, W. S., and Sullivan, J. K. (2009) *J. Bone Miner. Res.* **24,** 182–195
32. Li, J., Sarosi, I., Yan, X. Q., Morony, S., Capparelli, C., Tan, H. L., McCabe, S., Elliott, R., Scully, S., Van, G., Kaufman, S., Juan, S. C., Sun, Y., Tarpley, J., Martin, L., Christensen, K., McCabe, J., Kostenuik, P., Hsu, H., Fletcher, F., Dunstan, C. R., Lacey, D. L., and Boyle, W. J. (2000) *Proc. Natl. Acad. Sci. U.S.A.* **97,** 1566–1571
33. Bouxsein, M. L., Pierroz, D. D., Glatt, V., Goddard, D. S., Cavat, F., Rizzoli, R., and Ferrari, S. L. (2005) *J. Bone Miner. Res.* **20,** 635–643
34. Ferrari, S. L., Pierroz, D. D., Glatt, V., Goddard, D. S., Bianchi, E. N., Lin, F. T., Manen, D., and Bouxsein, M. L. (2005) *Endocrinology* **146,** 1854–1862
35. Turner, C. H., and Burr, D. B. (1993) *Bone* **14,** 595–608
36. Baldock, P. A., Sainsbury, A., Allison, S., Lin, E. J., Couzens, M., Boey, D., Enriquez, R., During, M., Herzog, H., and Gardiner, E. M. (2005) *J. Bone Miner. Res.* **20,** 1851–1857
37. Lacey, D. L., Timms, E., Tan, H. L., Kelley, M. J., Dunstan, C. R., Burgess, T., Elliott, R., Colombero, A., Elliott, G., Scully, S., Hsu, H., Sullivan, J., Hawkins, N., Davy, E., Capparelli, C., Eli, A., Qian, Y. X., Kaufman, S., Sarosi, I., Shalhoub, V., Senaldi, G., Guo, J., Delaney, J., and Boyle, W. J. (1998) *Cell* **93,** 165–176
38. Rogers, M. J., Gordon, S., Benford, H. L., Coxon, F. P., Luckman, S. P., Monkkonen, J., and Frith, J. C. (2000) *Cancer* **88,** 2961–2978
39. Weinstein, R. S., Roberson, P. K., and Manolagas, S. C. (2009) *N. Engl. J. Med.* **360,** 53–62
40. Ominsky, M., Jolette, J., Smith, S. Y., Vlasseros, F., Samadfam, R., and Kostenuik, P. J. (2008) *J. Bone Min. Res.* **23,** S61
41. Brown, J. P., Prince, R. L., Deal, C., Recker, R. R., Kiel, D. P., de Gregorio, L. H., Hadji, P., Hofbauer, L. C., Alvaro-Gracia, J. M., Wang, H., Austin, M., Wagman, R. B., Newmark, R., Libanati, C., San Martin, J., and Bone, H. G. (2009) *J. Bone Miner. Res.* **24,** 153–161
42. Cosman, F., Nieves, J., Zion, M., Woelfert, L., Luckey, M., and Lindsay, R. (2005) *N. Engl. J. Med.* **353,** 566–575
43. Cosman, F., Wermers, R. A., Recknor, C., Mauck, K. F., Xie, L., Glass, E. V., and Krege, J. H. (2008) *Calcif Tissue Int.* **82,** S59
44. Fox, J., Miller, M. A., Newman, M. K., Recker, R. R., Turner, C. H., and Smith, S. Y. (2007) *Bone* **41,** 321–330
45. Takahashi, H., Hattner, R., Epker, B. N., and Frost, H. M. (1964) *Henry Ford Hosp. Med. Bull.* **12,** 359–364
46. Ominsky, M. S., Schroeder, J., Jolette, J., Smith, S. Y., Farell, D. J., Atkinson, J. E., and Kostenuik, P. J. (2008) *J. Bone Min. Res.* **22,** S88
47. Ohishi, M., Chiusaroli, R., Ominsky, M., Asuncion, F., Thomas, C., Khatri, R., Kostenuik, P., and Schipani, E. (2009) *Am. J. Pathol.* **174,** 2160–2171